THE INFLUENCE OF EQUILIBRATION ON THE X-RAY INTENSITY OF SEDOV MODELS

D. Jerius and R. G. Teske
Department of Astronomy
University of Michigan
Ann Arbor, Michigan

Abstract: We have synthesized a set of SNR X-ray and coronal iron surface brightness profiles to determine observational constraints to help distinguish how the remnants' ion-electron energy equilibration time-scales compare to their ionization time-scales. The profiles are based on Sedov-Taylor blast wave models under the two scenarios (1) equal T_{ion} and T_e or (2) Coulomb equilibration of T_e and T_{ion}. Resultant spectra were convolved with *Einstein* HRI and IPC sensitivity curves to simulate satellite observations of actual remnants.

Introduction: Previous studies of X-ray emission from SNR's in the adiabatic phase have indicated the importance of the ion-electron energy equilibration process behind the shock front in determining the electron-ion temperature structure. Models of the Cygnus Loop (Raymond *et al.* 1983; Fesen and Itoh 1985) favor equipartition by Coulomb interactions while models for Tycho's remnant (Hamilton *et al.* 1986b) and SN1006 (Hamilton *et al.* 1986a) indicate the presence of a possible rapidly equilibrated component. Complicating the picture is the possibility of reverse shocks setting up electron populations of different temperatures. A cooler electron component is also present due to secondary ionizations.

In order to study these processes, we have synthesized a set of X-ray and forbidden coronal iron surface brightness profiles. Teske (1984) pointed out that the forbidden coronal iron lines are a good indicator of which equilibration process is at work. However, it is predicted that in most remnants the [Fe X] red line will be weak or undetectable even though the [Fe XIV] green line is detectable. In these cases, the X-ray emission might prove a suitable substitute for the red line. In addition, the difference in spectral sensitivity between the various imaging instruments might shed some light on the problem (Hamilton and Sarazin 1984) since the equilibration processes tend to produce distinguishable spectra.

Models: We have computed a set of blast wave models for the shock speeds v_s = 275, 400, 525, 650 km/s and n_o = 0.01, 0.1, 1 cm^{-3}. The models include time-dependent, non-equilibrium ionization of C, N, O, Ne, Mg, Si, S, Ca, Fe, Ni, Ar, Al, and Na. The models were used to generate X-ray spectra (both line and continuous emission) at 99 positions along a projected radius of a remnant. The spectra were then convolved with instrumental responses and interstellar extinction to produce synthetic surface brightness profiles. Similar profiles were produced for the two coronal lines.

https://doi.org/10.1017/S025292110010226X Published online by Cambridge University Press

Results: We find that at low shock speeds, profiles for the two equilibration processes are essentially identical. At higher speeds, the electron and ion temperatures grow more disparate in the Coulomb equilibration models, producing a lower degree of ionization and thus a softer spectrum behind the shock front in the Coulomb case. However, because the spectrum observed at a point in the remnant is the integral of the spectra at all points (at different radii) along that line of sight, the resultant brightness profiles depend upon conditions across the whole remnant. Geometrical factors can mask any differences.

Unfortunately the X-ray profiles for extinction free models (Fig. 1) are only slightly sensitive to the equilibration processes (their peak values varying by less than 50%), so that fitting observed profiles to models may not give dependable results. Since the *Einstein* IPC and HRI have different spectral sensitivities, a comparison of peak intensities as seen by the two instruments might lead to the differentiation of the equilibration processes. We find, however, that only in cases with interstellar extinction is there an appreciable difference, and then only for shocks with $v_s > 400$ km/s and low or moderate densities (Fig. 2).

The applicability of the iron line emissions to this problem depends on whether or not they are observable. Lucke *et al.* (1979) find a lower limit of detectibility of 2×10^{-8} erg cm^{-2} s^{-1} sr^{-1} by aperture photometry while Teske and Petre (1987) quote a limit of 1×10^{-7} ergs cm^{-2} s^{-1} sr^{-1} as done by CCD observations. In terms of the synthesized profiles, the [Fe X] line is observable only at lower shock speeds with $n_o > 0.2$ cm^{-3} (see Fig. 3). In this region the [Fe XIV] green line is observable for $400 \leq v_s \leq 650$ km/s (both of these predictions assume no interstellar extinction). Comparisons of peak iron to X-ray intensities indicate that they might differentiate between the equilibration process in this region. Ambiguities due to the influence of interstellar extinction on the X-ray emission may compromise this procedure, since shocks with different speeds and equilibration processes may mimic each other. We believe, however, that with high signal to noise observations or independent measurements of the shock speeds that the iron line intensities will prove invaluable. Examination of the spectra produced at the location of maximum X-ray emission reveals that several lines of N-like ions, Li-like Ne VIII and Ne-like Fe XVII are fairly sensitive to the equilibration process and may serve as yet another means of determining which process is at work.

Application to Observed Remnants: We have applied our X-ray models to two remnants, the Cygnus Loop and Puppis A. For the Cygnus Loop, we used the IPC data of Ku *et al.* (1984) and found that our best fit to the data used blast parameters determined by the optical study of Fesen and Itoh (1985); $v_s = 220$ km/s, $n_o = 0.54$ cm^{-3} and an interstellar column density of 4×10^{20} cm^{-2} (see Fig. 4). With these parameters, there is no distinction between the two types of equilibration. Our attempts to fit the data with Ku's parameters were not at all successful, leading us to believe that the IPC pulse-height spectrum is sensitive to different shock speeds than the integrated IPC radial profiles (mainly because the pulse-height spectrum emphasizes $E_{h\nu} \geq 0.2$ keV, which will favor higher speed shocks).

Data for Puppis A were kindly provided by R. Petre. We fitted a model to a radial cut taken through regions studied by Szymkowiak (1985) with the *Einstein* SSS, choosing a profile running across the shock front at position angle 42° through Szymkowiak's region N. We find that models using Szymkowiak's spectra-based parameters do not fit the radial profile very well. This is attributable to both departures in spherical symmetry in Puppis A and to the high probability that the ISM is non-uniform (Petre *et al.*, 1982; Teske and Petre 1987).

Conclusion: Preliminary comparisons of our X-ray models to published data have not produced a concrete differentiation between the two ion-electron energy equilibration processes. Comparisons with other data are planned. The additional information provided by further observations of SNR's in the forbidden coronal iron lines should provide enough information to distinguish these processes.

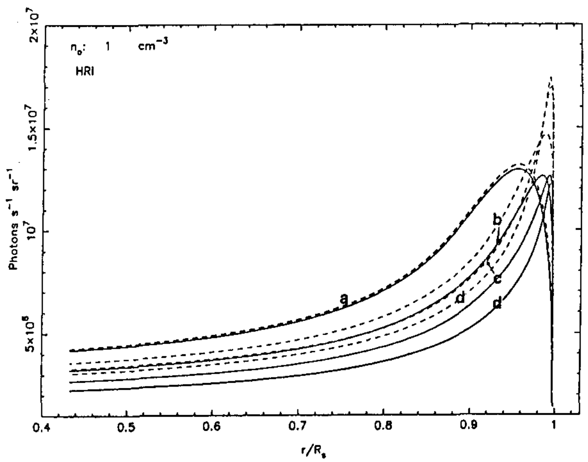

Fig 1. X-ray surface brightness profiles, no interstellar extinction. Solid curves; rapid equil. Dashed curves: Coulomb equil. Shock speeds: a 275 km/s; b 400 km/s; c 525 km/s; d 650 km/s.

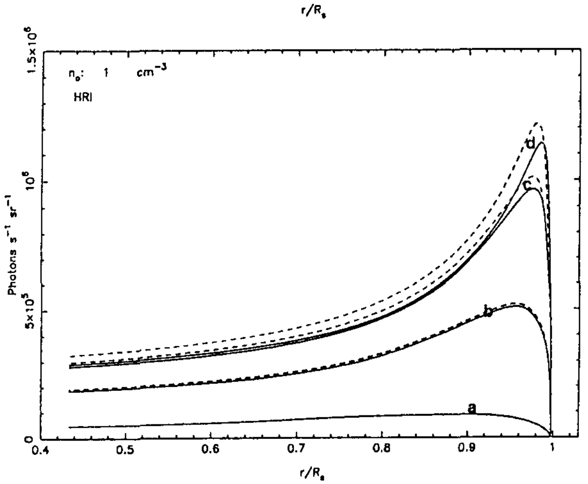

Fig 2. X-ray surface brightness profiles, with an interstellar column density of 3×10^{21} cm^{-2}. Other details are the same as in Figure 1.

https://doi.org/10.1017/S025292110010226X Published online by Cambridge University Press

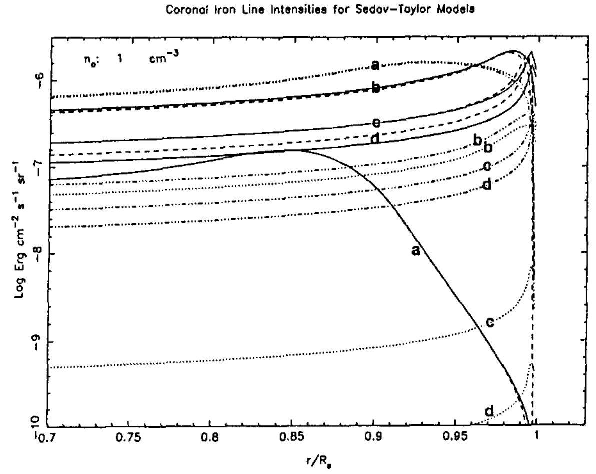

Fig 3. Forbidden coronal iron surface brightness profiles. Solid: [Fe XIV], rapid equil. Dashed: [Fe XIV], Coulomb equil. Dotted: [Fe X], rapid equil. Dash-dotted: [Fe X], Coulomb equil. Shock speeds are labelled as in Figure 1.

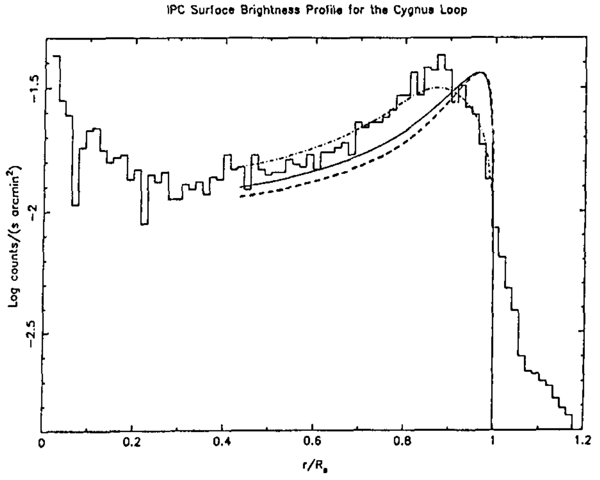

Fig 4. Theoretical IPC profiles for the Cygnus Loop. Histogram: Data of Ku *et al.* (1984). Models with Ku's parameters -- solid curve: Coulomb equil.; dashed: rapid equil. Model with V_s = 220 km/s, n_o = 0.54 cm^{-3} -- dash-dot curve.

References

Fesen, R. A., and Itoh, H. 1985, *Ap. J.*, 295, 43.
Hamilton, A.J. S., and Sarazin, C. L., 1984, *Ap. J.*, 284, 601.
Hamilton, A. J. S., Sarazin, C. L., and Szymkowiak, A. E., 1986a, *Ap. J.*, 300, 698.
Hamilton, A. J. S., Sarazin, C. L., and Szymkowiak, A. E. 1986b, *Ap. J.*, 300, 713.
Ku, W. H.-M., Kahn, S. M., Pisarski, R., and Long, K. S. 1984, *Ap. J.*, 278, 615.
Lucke, R. L., Zarnecki, J. C., Woodgate, B. E., Culhane, J. L., and Socker, D. G., 1979, *Ap. J.*, 228, 615.
Raymond, J. C., Blair, W. P., Fesen, R. A., and Gull, T. R. 1983, *Ap. J.*, 275, 636.
Szymkowiak, A. E. 1985, "X-Ray Spectra of Supernova Remnants", NASA Technical Memorandum 86169.
Teske, R. G. 1984, *Ap. J.*, 277, 832.
Teske, R. G., and Petre, R. 1987, *Ap. J.*, 314, 673.